

RIEMANNIAN MANIFOLDS DUAL TO STATIC SPACETIMES

Carolina Figueiredo and José Natário

ABSTRACT. In this paper we establish a one-to-one correspondence between static spacetimes and Riemannian manifolds that maps causal geodesics to geodesics, as suggested by Epstein. We explore constant curvature spacetimes – such as the de Sitter and Anti-de Sitter spacetimes – and conclude that they map to constant curvature Riemannian manifolds, namely the Euclidean space, the sphere or the hyperbolic space. By imposing the conditions required to obtain the sphere, we deduce the metrics for which there is radial oscillatory motion with period independent of the amplitude and the corresponding perfect fluid stress tensors. Finally, we give examples of surfaces corresponding to certain types of motion for metrics which do not exhibit constant curvature such as Schwarzschild, Schwarzschild De Sitter, Schwarzschild Anti-de Sitter and even for a simplified model of a wormhole.

INTRODUCTION

When dealing with static spacetimes, the metric can be reduced to the following form:

$$ds^2 = -e^{2\Phi(x^1, x^2, x^3)} dt^2 + \gamma_{ij}(x^1, x^2, x^3) dx^i dx^j \quad (1)$$

where γ stands for a 3-dimensional Riemannian metric.

In [2] L. C. Epstein suggested that for time-like separated events, one would get a Riemannian metric by rewrite (1) as

$$dt^2 = e^{-2\Phi} (d\tau^2 + \gamma_{ij} dx^i dx^j) \quad (2)$$

where $d\tau^2 = -ds^2$ is the proper time interval. Note that τ is now a coordinate function while t is the arclength.

This establishes a one-to-one correspondence between static spacetimes and Riemannian manifolds, both with the same topology, $\mathbb{R} \times \Sigma$, where Σ is a 3-manifold. In this note we prove that this correspondence maps causal geodesics to geodesics and use it to explore the properties of the spacetimes.

1. GEODESIC CORRESPONDENCE

We now prove the equivalence between the geodesics of the Lorentzian metric (1) and the Riemannian metric (2) obtained as described above. If we start with a 5-dimensional metric¹

$$ds^2 = -e^{2\Phi} dt^2 + \gamma_{ij} dx^i dx^j + d\tau^2, \quad (3)$$

and choose the coordinate time, t , as the parameter, then its null geodesics, $ds^2 = 0$, are the Fermat's metric geodesics [4]

$$dt^2 = e^{-2\Phi} (\gamma_{ij} dx^i dx^j + d\tau^2), \quad (4)$$

¹This idea is similar to the Eisenhart lift [1].

which is, in fact, the Epstein metric (2). Furthermore, since the metric (4) is the product of the Lorentzian metric (1) by $d\tau^2$, the projection of the 5-dimensional geodesics on the submanifolds of constant τ (parametrized by (t, x^i)) are the geodesics of the Lorentzian metric (1). Therefore both sets of geodesics coincide.

2. CONSTANT CURVATURE SPACETIMES

Now we apply this result to constant curvature spacetimes and conclude that these lead us to constant curvature Riemannian manifolds.

2.1 Minkowski Spacetime

The metric of the flat Minkowski spacetime is given by

$$ds^2 = -dt^2 + dx^2 + dy^2 + dz^2, \quad (5)$$

choosing units properly so that $c = 1$. Applying Epstein's idea to this spacetime leads us to the following Riemannian manifold:

$$dt^2 = d\tau^2 + dx^2 + dy^2 + dz^2. \quad (6)$$

This is trivially the 4-dimensional Euclidean plane. Consequently, the geodesics of our Riemannian manifold are straight lines, and so, motions in this spacetime satisfy: $\frac{d\tau}{dt} \propto \frac{dx}{dt} \propto \frac{dy}{dt} \propto \frac{dz}{dt}$.

2.2 Rindler Spacetime

Applying Epstein's idea to Rindler's spacetime

$$ds^2 = -z^2 dt^2 + dx^2 + dy^2 + dz^2, \quad (7)$$

which is a flat space, $S = 0$, leads us to the following Riemannian metric:

$$dt^2 = \frac{1}{z^2} (d\tau^2 + dx^2 + dy^2 + dz^2). \quad (8)$$

This is the 4-dimensional hyperbolic space. Note that, this is an example in which this process turns out to be quite unpredictable. Starting with a flat space, $S = 0$, the resulting Riemannian metric corresponds to the hyperbolic space, $S < 0$. As a result, the geodesics of Rindler spacetime correspond to the geodesics of the hyperbolic space given by (8).

2.3 De Sitter Spacetime

The metric of the de Sitter spacetime, $\Lambda > 0$, is given by

$$ds^2 = -\left(1 - \frac{\Lambda}{3}r^2\right) dt^2 + \left(1 - \frac{\Lambda}{3}r^2\right)^{-1} dr^2 + r^2 d\Omega^2, \quad (9)$$

and has scalar curvature $S = 4\Lambda$. Notice that $d\Omega^2$ stands for the S^2 metric, $d\Omega^2 = d\theta^2 + \sin^2\theta d\phi^2$. Applying Epstein's idea to this spacetime yields

$$dt^2 = \left(1 - \frac{\Lambda}{3}r^2\right)^{-1} \left[d\tau^2 + \left(1 - \frac{\Lambda}{3}r^2\right)^{-1} dr^2 + r^2 d\Omega^2 \right]. \quad (10)$$

This Riemannian metric has negative scalar curvature $S = -4\Lambda$. According to Killing-Hopf theorem, locally this manifold must match the 4-dimensional hyperbolic space. If one writes the 5-dimensional Minkowski spacetime as the Cartesian product of the 3-dimensional Euclidean space and Milne 2-dimensional spacetime as follows

$$dt^2 = -d\rho^2 + \rho^2 d\tau^2 + dr^2 + r^2 d\Omega^2, \quad (11)$$

then one can obtain the 4-dimensional hyperbolic space by considering

$$\rho^2 - r^2 = 1 \Leftrightarrow \begin{cases} r = \sinh u \\ \rho = \cosh u \end{cases}, \quad (12)$$

which leads us to $dr^2 - d\rho^2 = du^2$ and consequently

$$dt^2 = du^2 + \cosh^2 u d\tau^2 + \sinh^2 u d\Omega^2. \quad (13)$$

This metric may also be obtained from (10) by setting $\Lambda = 3$ and $\frac{dr}{1-r^2} = du \Leftrightarrow u = \operatorname{arctanh} r \Leftrightarrow \tanh u = r$.

2.4 Plane Anti-de Sitter

Applying Epstein's idea to the spacetime

$$ds^2 = \frac{\Lambda}{3} r^2 dt^2 + \left(-\frac{\Lambda}{3} r^2\right)^{-1} dr^2 + r^2 (dx^2 + dy^2), \quad (14)$$

where $\Lambda < 0$ stands for the cosmological constant, leads us to the following Riemannian manifold:

$$dt^2 = \frac{3}{\Lambda r^2} \left[-d\tau^2 + \frac{3}{r^2 \Lambda} dr^2 - r^2 (dx^2 + dy^2) \right]. \quad (15)$$

The Riemann tensor of this metric can be computed to be zero. Therefore, accounting the Killing-Hopf theorem, the manifold obtained must be isometric to the 4-dimensional Euclidean space in some coordinates. In fact, taking $\Lambda = -3$ (by choosing convenient units) and defining $u = \frac{1}{r}$, one can rewrite the Epstein metric in the following way:

$$dt^2 = du^2 + u^2 d\tau^2 + dx^2 + dy^2. \quad (16)$$

This is the product of the metric for the 2-dimensional plane in polar coordinates, where τ is the angular coordinate, and another 2-dimensional plane, which is isometric to the 4-dimensional Euclidean space. Hence the geodesics of our Riemannian manifold are straight lines. As a result, we may conclude that motions in this spacetime are such that $\frac{du}{dt}$, $u \frac{d\tau}{dt}$, $\frac{dx}{dt}$ and $\frac{dy}{dt}$ are proportional.

2.5 Hyperbolic Anti-de Sitter

The metric of the hyperbolic Anti-de Sitter spacetime, $\Lambda < 0$, is given by

$$ds^2 = \left(1 + r^2 \frac{\Lambda}{3}\right) dt^2 - \left(1 + r^2 \frac{\Lambda}{3}\right)^{-1} dr^2 + r^2 d\theta^2 + r^2 \sinh^2 \theta d\phi^2, \quad (17)$$

and has constant scalar curvature $S = 4\Lambda$. The resulting Riemannian metric is the following:

$$dt^2 = - \left(1 + r^2 \frac{\Lambda}{3}\right)^{-1} \left[- \left(1 + r^2 \frac{\Lambda}{3}\right)^{-1} dr^2 + r^2 (d\theta^2 + \sinh^2 \theta d\phi^2) + d\tau^2 \right]. \quad (18)$$

Computing the Riemann tensor we can see that this metric has constant curvature, and constant negative scalar curvature $S = 4\Lambda$. Thus, taking again into consideration the Killing-Hopf theorem, the resulting Riemannian manifold should be isometric to the 4-dimensional hyperbolic space. If one writes the metric of a Lorentzian manifold corresponding to the Cartesian product of the 2-plane and the Minkowski 1+2 spacetime in the form

$$dt^2 = dr^2 + r^2 d\tau^2 - d\rho^2 + \rho^2 (d\theta^2 + \sinh^2 \theta d\phi^2), \quad (19)$$

then the 4-dimensional hyperbolic space is given by

$$\rho^2 - r^2 = 1 \Leftrightarrow \begin{cases} r = \sinh u \\ \rho = \cosh u \end{cases}, \quad (20)$$

which yields $dr^2 - d\rho^2 = du^2$ and thus

$$dt^2 = du^2 + \sinh^2 u d\tau^2 + \cosh^2 u (d\theta^2 + \sinh^2 \theta d\phi^2). \quad (21)$$

This, in fact, is what follows from (18) by setting $\Lambda = -3$ and $\frac{dr}{1-r^2} = du \Leftrightarrow u = \operatorname{arctanh} r \Leftrightarrow \tanh u = r$.

2.6 Spherical Anti-de Sitter

The metric of spherical Anti-de Sitter spacetime is given by

$$ds^2 = - \left(1 - r^2 \frac{\Lambda}{3}\right) dt^2 + \left(1 - r^2 \frac{\Lambda}{3}\right)^{-1} dr^2 + r^2 d\Omega^2, \quad (22)$$

and has scalar curvature $S = 4\Lambda$. This lead us to the following Riemannian metric:

$$dt^2 = \left(1 - r^2 \frac{\Lambda}{3}\right)^{-1} \left[d\tau^2 + \left(1 - r^2 \frac{\Lambda}{3}\right)^{-1} dr^2 + r^2 d\Omega^2 \right]. \quad (23)$$

Computing the Riemann tensor we can see that this metric has constant curvature, and constant positive scalar curvature $S = -4\Lambda$. By the Killing Hopf theorem, the resulting Riemannian manifold should be 4-sphere S^4 . Indeed, the Euclidean metric of \mathbb{R}^5 can be written as

$$dt^2 = dr^2 + r^2 d\tau^2 + d\rho^2 + \rho^2 d\Omega^2 \quad (24)$$

and S^4 is simply given by:

$$r^2 + \rho^2 = 1 \Leftrightarrow \begin{cases} r = \cos u \\ \rho = \sin u \end{cases} \quad \left(0 < u < \frac{\pi}{2}\right). \quad (25)$$

This yields $dr^2 + d\rho^2 = du^2$, and therefore

$$dt^2 = du^2 + \cos^2 u d\tau^2 + \sin^2 u d\Omega^2, \quad (26)$$

which is exactly the metric obtained in (23) by setting $\Lambda = -3$ and $\frac{dr}{1+r^2} = du \Leftrightarrow u = \arctan r \Leftrightarrow \tan u = r$. Therefore the geodesics of this spacetime are simply the geodesics of S^4 , which are great circles.

3. RADIAL ISOCHRONOUS OSCILLATORY MOTION

The results in section 2.6, relating the geodesics of the spherical ADS spacetime and the S^4 , show that in this spacetime θ and r should be periodic in time whereas τ and ϕ should monotonically increasing. This means that the motions in the spherical ADS spacetime are periodic in space and isochronous, that is, they all have the same period as measured by proper time. Moreover, since all great circles have the same length 2π they also have the same period as measured by the coordinate time.

In particular, radial oscillatory motion, obtained by setting $d\theta = d\phi = 0$, correspond to geodesics of S^2 , with the usual round metric

$$dt^2 = du^2 + \cos^2 u d\tau^2. \quad (27)$$

The Epstein metric can be used to investigate similar isochronous radial oscillatory motion in arbitrary static spherically symmetric spacetimes. Starting the Lorentzian metric

$$ds^2 = -e^{2\Phi} dt^2 + e^{2\Lambda} dr^2 + r^2 d\Omega^2, \quad (28)$$

the resulting Riemannian metric is given by:

$$dt^2 = e^{-2\Phi} d\tau^2 + e^{2(\Lambda-\Phi)} dr^2 + e^{-2\Phi} r^2 d\Omega^2, \quad (29)$$

and so, in order to obtain (27), we must have

$$\begin{cases} e^{2(\Lambda-\Phi)} dr^2 = du^2 \\ \cos^2 u = e^{-2\Phi} \end{cases} \Leftrightarrow \begin{cases} \frac{du}{dr} = e^{\Lambda-\Phi} \\ \cos u = e^{-\Phi} \end{cases}, \quad e^{-\Phi} \in [0, 1]. \quad (30)$$

Differentiating the second equation with respect to r we obtain

$$\sin uu' = \Phi' e^{-\Phi} \Leftrightarrow e^{\Lambda} \sqrt{1 - e^{-2\Phi}} = \Phi' \Leftrightarrow e^{\Lambda} = \frac{\Phi' e^{\Phi}}{\sqrt{e^{2\Phi} - 1}}, \quad (31)$$

which gives us the relation between e^{Λ} and e^{Φ} .

For the spherically symmetric metric (28), the Einstein tensor reduces to [5]

$$G_{tt} = \frac{e^{2\Phi}}{r^2} \left[1 + e^{-2\Lambda} (2r\Lambda' - 1) \right], \quad (32)$$

$$G_{rr} = \frac{1}{r^2} \left(1 - e^{2\Lambda} \right) + \frac{2\Phi'}{r}, \quad (33)$$

$$G_{\theta\theta} = r^2 e^{-2\Lambda} \left(\Phi'' + \Phi'^2 + \frac{\Phi'}{r} - \Phi' \Lambda' - \frac{\Lambda'}{r} \right), \quad (34)$$

$$G_{\phi\phi} = \sin^2 \theta G_{\theta\theta}, \quad (35)$$

where $'$ stands for $\frac{d}{dr}$ and all other components vanish.

When implementing the extra condition (31), it is useful to change of coordinates. Defining

$$e^{\Phi} = \cosh \psi, \quad (36)$$

equation (31) leads to

$$\psi' = e^{\Lambda} \Rightarrow \psi = \int_0^r e^{\Lambda(s)} ds. \quad (37)$$

For a general diagonal stress-energy tensor, which is given by

$$T_{tt} = \rho e^{2\Phi}, \quad (38)$$

$$T_{rr} = p_r e^{2\Lambda}, \quad (39)$$

$$T_{\theta\theta} = r^2 p_\theta, \quad (40)$$

$$T_{\phi\phi} = \sin^2 \theta T_{\theta\theta}, \quad (41)$$

where ρ stands for the energy density, p_r is the radial pressure and p_θ the tangential pressure. Einstein's equations are given by

$$\frac{1}{r^2} \left[1 + \frac{1}{\psi'} \left(\frac{2r\psi''}{\psi'} - 1 \right) \right] = 8\pi\rho, \quad (42)$$

$$\frac{1 - \psi'^2}{r^2} + \frac{2\psi' \tanh \psi}{r} = 8\pi p_r \psi'^2, \quad (43)$$

$$\frac{1}{\psi'^2} \left(\psi'^2 + \frac{\psi' \tanh \psi}{r} - \frac{\psi''}{\psi' r} \right) = 8\pi p_\theta. \quad (44)$$

(The resulting equation for $G_{\phi\phi}$ is exactly the same as the one for $G_{\theta\theta}$ and, therefore, it is omitted above).

These equations give the energy density, radial pressure and tangential pressure of the matter generating a spacetime in which there are radial isochronous oscillatory motions. Notice that the choice of $\psi(r)$ is arbitrary, and determines the metric through (36) and (37).

3.1 Perfect Fluid

For the case of a perfect fluid, we must have $p_r = p_\theta$, and so by (43) and (44), ψ must satisfy

$$-\psi'^3 + \psi' + r\psi'^2 \tanh \psi - r^2\psi'^3 + \psi''r = 0. \quad (45)$$

Numerically solving this equation leads us to various solutions for $\psi(r)$, $\psi'(r)$ and, consequently, for $e^{\Lambda(r)}$. However, only a one-parameter family of these solutions satisfy the condition that both radial pressure and density remain finite at the center of the star. Below we present two of these solutions and the corresponding $p_r(r)$ and $\rho(r)$ profiles. In both cases the initial values for the numerical solution were given at $r = 0.75$. The result presented ranges from $r = 0.001$ to $r = 0.75$.

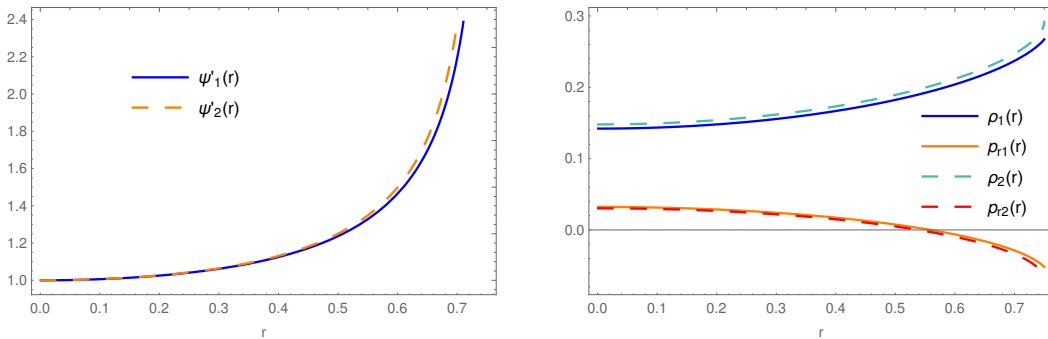


Figure 1: ψ'_1 : $\psi_1(0.75) = 0.99$, $\psi'_1(0.75) = 4.9915$; ψ'_2 : $\psi_1(0.75) = 1.078$, $\psi'_1(0.75) = 749$

Looking at the second plot, one can check that both solutions satisfy the dominant energy condition, $\rho > |p|$, and, in both cases, p_r vanishes at a certain value of r , as expected. However, the second plot shows that density grows as radial pressure decreases. This means that the equation of state, $p = p(\rho)$, will be such that $\frac{dp}{d\rho} < 0$ and, consequently, the star is unstable. Since we found this behaviour in all the numerical solutions obtained, we conclude that only unstable stars may give rise to this type of oscillatory motion.

3.2 Einstein Cluster

Einstein Cluster is a class of solutions to Einstein's equations which models a cloud of massive particles following circular geodesics acted by their collective gravitational field. In this system the radial pressure, p_r , vanishes and so equation (43) reduces to:

$$\frac{1 - \psi'^2}{r^2} + \frac{2\psi' \tanh \psi}{r} = 0. \quad (46)$$

Numerically solving this differential equation leads us to a single physically meaningful solution (in which all physical quantities remain finite) for each radius chosen to give the initial value. In the plot below, we present the solution in which the initial value is given at $r = 0.5$ and the corresponding $p_\theta(r)$ and $\rho(r)$ profiles.

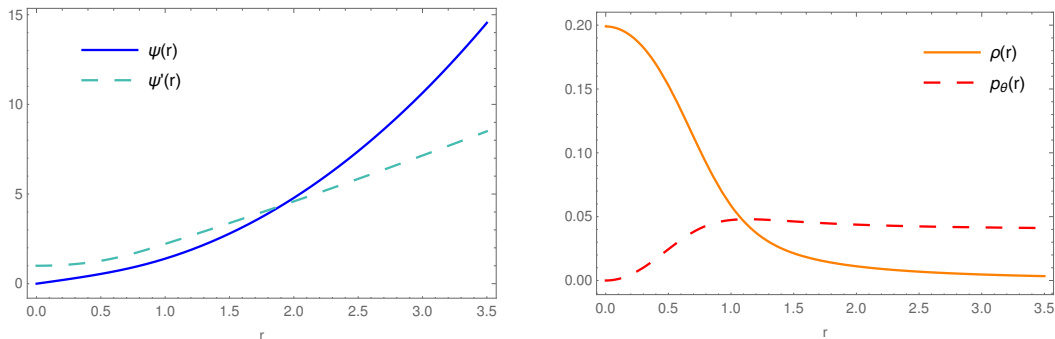


Figure 2: $\psi(0.5) = 0.54462$

Since we are now dealing with tangential pressure, there is no longer any restriction regarding the behaviour of this variable. Therefore, the result obtained allows us to conclude that for an Einstein Cluster, with pressure and density profiles as the ones obtained, allows radial isochronous oscillatory motion.

4. NON-CONSTANT CURVATURE SPACETIMES

We will now explore the properties of the Epstein's Riemannian manifolds in other spacetimes which do not exhibit constant curvature.

4.1 Schwarzschild's Spacetime

The Schwarzschild solution describes the gravitational field produced by a spherical body of mass m :

$$ds^2 = - \left(1 - \frac{2m}{r}\right) dt^2 + \left(1 - \frac{2m}{r}\right)^{-1} dr^2 + r^2 d\Omega^2. \quad (47)$$

This metric has vanishing Ricci tensor (and, consequently vanishing scalar curvature). Taking into account the results of section 2, one might expect that the resulting Epstein metric,

$$dt^2 = \left(1 - \frac{2m}{r}\right)^{-1} \left[d\tau^2 + \left(1 - \frac{2m}{r}\right)^{-1} dr^2 + r^2 d\Omega^2 \right], \quad (48)$$

would also have vanishing Ricci tensor. However, this is not the case, it has a diagonal non-zero Ricci tensor and scalar curvature $S = -\frac{12m^2}{r^4}$. Thus we are not able to easily visualize the shape of the manifold and consequently its geodesics. Notwithstanding, since we are working with a Riemannian manifold, one can still study the surfaces resulting from certain types of motion.

Null Geodesics

For example, for the motion of a light ray, $d\tau^2 = 0$, in the equatorial plane, $\theta = \frac{\pi}{2} \Rightarrow d\theta^2 = 0$, the metric reduces to

$$dt^2 = \left(1 - \frac{2m}{r}\right)^{-1} \left[\left(1 - \frac{2m}{r}\right)^{-1} dr^2 + r^2 d\phi^2 \right]. \quad (49)$$

In order to visualize the resulting manifold one must use cylindrical coordinates so that $\rho^2 = \left(1 - \frac{2m}{r}\right)^{-1} r^2$ and $d\rho^2 + dz^2 = \left(1 - \frac{2m}{r}\right)^{-2} dr^2$. From the second condition, one can find $\frac{dz}{dr}$ and therefore extract $z(r)$. The result obtained for unitary mass, $m = 1$, is presented in figure 3.

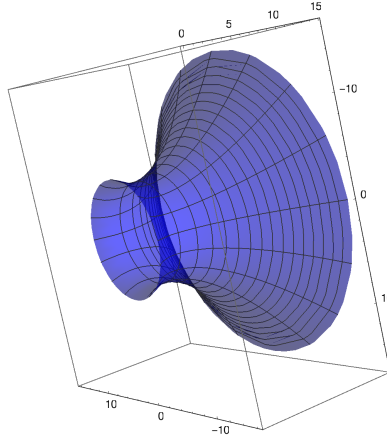


Figure 3: *Schwarzschild Spacetime ; $d\tau = d\theta = 0$*

As expected the resulting manifold is a surface of revolution. Therefore, $\rho = f(z)$, being f an unknown function, and consequently, $ds^2 = f(z)^2 d\phi^2 + (f'^2(z) + 1) dz^2$. Finding the Lagrangean of this motion leads us to $L = \frac{1}{2} (f^2(z) \dot{\phi}^2 + (f'^2(z) + 1) \dot{z}^2)$. Since ϕ is a cyclic

coordinate, one can easily identify the effective potential of the system: $U_{eff} = \frac{l_\phi}{f^2(z)}$, with l_ϕ the conserved momenta in ϕ . The depression observed in the plot corresponds to a maximum of U_{eff} and, thus, to an unstable orbit. This suggests that there is a periodic motion in ϕ at $\frac{d\rho}{dr} = 0 \Leftrightarrow r = 3m$. Indeed, this orbit corresponds to the well known photon sphere. It is such that any small perturbation leads to motion either towards infinity or the black hole. If there is motion in ϕ , it is given by geodesics that curl around our surface. Contrarily, if there is no angular momenta, then this motion corresponds to the meridians of the surface.

Radial Motion

Additionally, one can also visualize the surface resulting from radial motion, $d\theta = d\phi = 0$. Defining ρ and z such that: $\rho^2 = \left(1 - \frac{2m}{r}\right)^{-1}$ and $d\rho^2 + dz^2 = \left(1 - \frac{2m}{r}\right)^{-2} dr^2$, under the conditions previously mentioned, one obtains the surface depicted in figure 4.

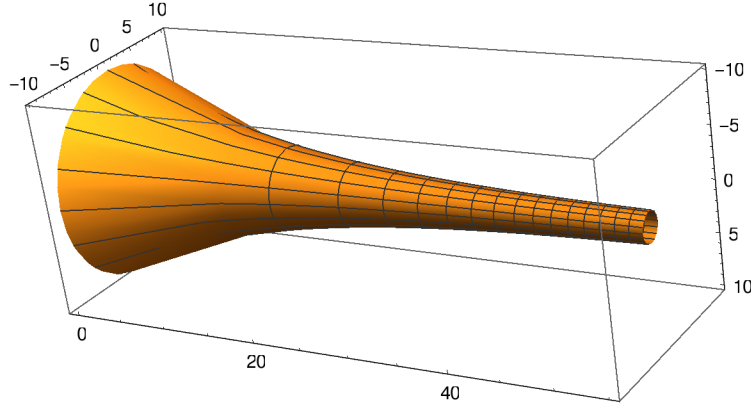


Figure 4: *Schwarzschild Spacetime ; $d\theta = d\phi = 0$*

Since there is no depression, the possible trajectories for free particles correspond to geodesics that curl around the surface. When $t \rightarrow \pm\infty$, they satisfy either $\rho \rightarrow \infty$, which corresponds to the black hole event horizon, or $\rho \rightarrow 1$, which corresponds to spacial infinity. Trajectories of light rays correspond to geodesics that do not curl around the surface since $d\tau^2 = 0$ but instead, go straight from the event horizon to infinity or vice-versa (the black lines in the plot). Note that, in the limit of being far from the black hole, the surface resembles a flat cylinder, as might be expected, since it must approach the Minkowski spacetime.

4.2 Interior Solution

A possible interior solution for the Schwarzschild spacetime is one for constant density, given by the metric

$$ds^2 = - \left[\frac{3}{2} \left(1 - \frac{2m}{R} \right)^{\frac{1}{2}} - \frac{1}{2} \left(1 - \frac{2m}{R^3} r^2 \right)^{\frac{1}{2}} \right]^2 dt^2 + \left(1 - \frac{2m}{R^3} r^2 \right) dr^2 + r^2 d\Omega^2, \quad (50)$$

where R stands for the radius of the spherical body. The resulting Riemannian metric is given by:

$$dt^2 = \left[\frac{3}{2} \left(1 - \frac{2m}{R} \right)^{\frac{1}{2}} - \frac{1}{2} \left(1 - \frac{2m}{R^3} r^2 \right)^{\frac{1}{2}} \right]^{-2} \left[d\tau^2 + \left(1 - \frac{2m}{R^3} r^2 \right) dr^2 + r^2 d\Omega^2 \right]. \quad (51)$$

Null geodesics

For the global solution of the motion of a light ray in the equatorial plane, one must set $d\theta = d\tau = 0$ and choose ρ and z so that: $\rho^2 = \left[\frac{3}{2} \left(1 - \frac{2m}{R} \right)^{\frac{1}{2}} - \frac{1}{2} \left(1 - \frac{2m}{R^3} r^2 \right)^{\frac{1}{2}} \right]^{-2} r^2$ and $d\rho^2 + dz^2 = \left[\frac{3}{2} \left(1 - \frac{2m}{R} \right)^{\frac{1}{2}} - \frac{1}{2} \left(1 - \frac{2m}{R^3} r^2 \right)^{\frac{1}{2}} \right]^{-2} \left(1 - \frac{2m}{R^3} r^2 \right) dr^2$. The surface obtained setting $R = 2.8$ and $m = 1$ is presented in figure 5.

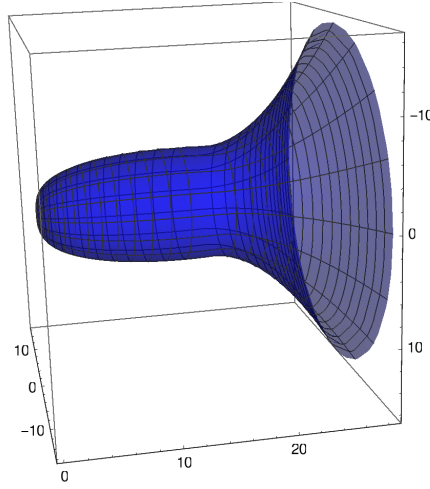


Figure 5: *Global Solution ; $d\tau = d\theta = 0$*

The meridians of this surface, the black lines in the plot, correspond to the motion of light beams with no angular momenta $d\phi = 0$, that simply go through our star. Looking at the shape of this surface, one may conclude that the coordinate time necessary to cross the star that is the length of the geodesic is larger than it would be in a flat space. This corresponds to well known Shapiro effect [6]. If there is motion in ϕ , the geodesics are curves that curl around the surface until $z = 0$ and then curl back towards infinity. Lastly, one can still find the depression previously identified at $r = 3m$, which matches an unstable circular orbit. But now, any small perturbation towards the centre will lead to a new geodesic that curls around the surface towards $\rho = 0$ and then returns back to $r = 3m$, taking infinite time to complete this cycle.

Radial Motion

Setting $d\theta = d\phi = 0$ and defining ρ and z such that: $\rho^2 = \left[\frac{3}{2} \left(1 - \frac{2m}{R} \right)^{\frac{1}{2}} - \frac{1}{2} \left(1 - \frac{2m}{R^3} r^2 \right)^{\frac{1}{2}} \right]^{-2}$ and $d\rho^2 + dz^2 = \left[\frac{3}{2} \left(1 - \frac{2m}{R} \right)^{\frac{1}{2}} - \frac{1}{2} \left(1 - \frac{2m}{R^3} r^2 \right)^{\frac{1}{2}} \right]^{-2} \left(1 - \frac{2m}{R^3} r^2 \right) dr^2$, one can obtain the global solution for radial motion. The result choosing $R = 3$ and $m = 1$ is shown in figure 6.

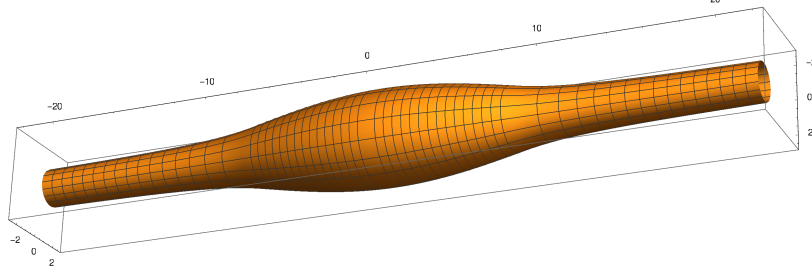


Figure 6: *Global Solution ; $d\theta = d\phi = 0$*

In addition to the geodesics identified in section 4.1, the interior solution considered introduces new possibilities of motion. Regarding only the surface of revolution corresponding to the interior solution, for $z = 0$, $\rho = f(z)$ reaches a maximum. Defining the Lagrangean $L = \frac{1}{2} (f^2(z)\dot{\tau}^2 + (f'(z)^2 + 1) \dot{z}^2)$, as previously, one can conclude that the effective potential, $U_{eff} = \frac{l_\tau}{f^2(z)}$ as a minimum at $z = 0$. Consequently, there is a stable circular orbit at $z = 0$. Since $dt^2 = f(0)d\tau^2$, this represents the situation of a particle at rest in the centre of our star. Any small perturbation leads to oscillatory motion represented by lines continuously curling around the surface centered at $z = 0$. This type of motion corresponds to radial oscillations near the centre of our massive body. If, however, the perturbation is strong enough to overcome the gravitational force, then the motion is given by geodesics that curl around our surface approaching infinity. Null geodesics, the motion of light beams, match the black lines in the plot. Since $d\tau = 0$, there is no angular motion around the surface and, therefore, light beams simply go through our massive body.

4.3 Schwarzschild de Sitter

The Schwarzschild de Sitter spacetime, $\Lambda > 0$, includes both a black hole event horizon and a cosmological horizon. As expected, the metric of this spacetime does not exhibit constant curvature and can be written as

$$ds^2 = - \left(1 - \frac{2m}{r} - \frac{\Lambda}{3} r^2 \right) dt^2 + \left(1 - \frac{2m}{r} - \frac{\Lambda}{3} r^2 \right)^{-1} dr^2 + r^2 d\Omega^2, \quad (52)$$

which leads us to a Riemannian metric given by:

$$dt^2 = \left(1 - \frac{2m}{r} - \frac{\Lambda}{3} r^2 \right)^{-1} \left[d\tau^2 + \left(1 - \frac{2m}{r} - \frac{\Lambda}{3} r^2 \right)^{-1} dr^2 + r^2 d\Omega^2 \right] \quad (53)$$

Radial Motion

Setting $d\theta = d\phi = 0$ and defining ρ and z such that: $\rho^2 = \left(1 - \frac{2m}{r} - \frac{\Lambda}{3} r^2 \right)^{-1}$ and $d\rho^2 + dz^2 = \left(1 - \frac{2m}{r} - \frac{\Lambda}{3} r^2 \right)^{-2} dr^2$, for $m = 0.1$ and $\Lambda = 3$, one obtains the surface presented in figure 7.

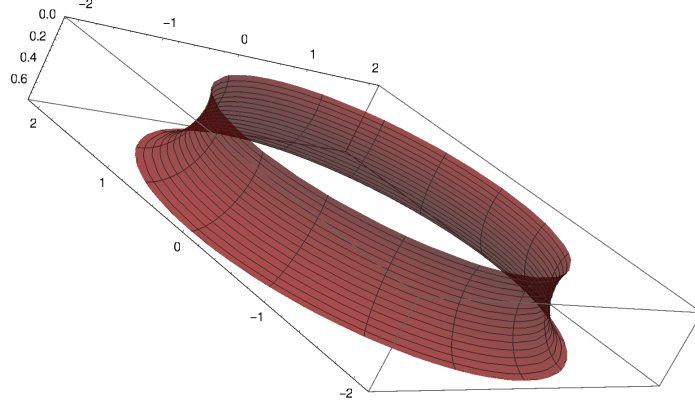


Figure 7: *Schwarzschild de Sitter spacetime ; $d\theta = d\phi = 0$*

Looking at the plot, one can easily see that the surface of revolution obtained for radial motion in the Schwarzschild de Sitter spacetime also presents a depression, which stands for an unstable equilibrium, at $\frac{d\rho}{dr} = 0 \Leftrightarrow r = \left(\frac{3m}{\Lambda}\right)^{\frac{1}{3}}$. This is due to the repulsive character of the positive cosmological constant. At $r = \left(\frac{3m}{\Lambda}\right)^{\frac{1}{3}}$, the repulsive cosmological force balances the attractive gravitational force created by the massive body. Any small perturbation leads either to motion towards the black hole horizon or the cosmological horizon given by geodesics that curl around our surface. For light rays, $d\tau = 0$, the geodesics are again the meridians of our surface, represented by the black lines in the plot, going either towards the black hole horizon or the cosmological horizon.

4.4 Schwarzschild Anti-de Sitter

The Schwarzschild Anti-de Sitter spacetime is given by the exact same metric of Schwarzschild de Sitter except for the fact that now $\Lambda < 0$.

Radial Motion

Following the previous procedure, for $m = 0.1$ and $\Lambda = -3$, one obtains the manifold depicted in figure 8, where the hole found on the top is actually just a missing point corresponding to infinity.

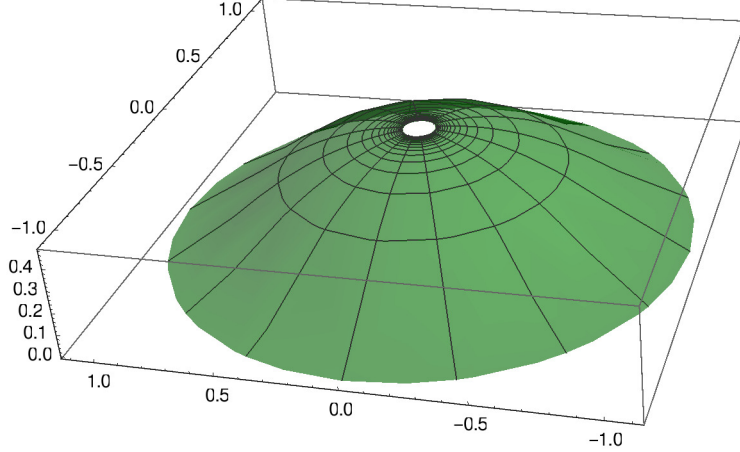


Figure 8: *Schwarzschild Anti-de Sitter spacetime ; $d\theta = d\phi = 0$*

For a negative cosmological constant there is no sign of unstable orbits. Light rays correspond to geodesics given by the black lines, $d\tau = 0$, and so they travel either from the massive body towards infinity or the other way around. Contrarily, particles moving slower than light may move towards infinity but will eventually return to $z = 0$. This is due to the attractive character of the Schwarzschild Anti-de Sitter spacetime, as in this case both the massive body and the cosmological constant attract the massive bodies towards $z = 0$.

4.5 Wormholes

According to [3], the spacetime metric that describes a static and spherically symmetric wormhole has the form

$$ds^2 = -e^{2\Phi(r)} dt^2 + \frac{dr^2}{1 - \frac{b(r)}{r}} + r^2 d\Omega^2, \quad (54)$$

where $\Phi(r)$ and $b(r)$ are arbitrary functions of r , the radial coordinate. While $\Phi(r)$ describes the gravitational redshift, $b(r)$ determines the shape of the wormhole. The radial coordinate ranges from r_0 , the wormhole's throat, to a , the wormhole's mouth. At $r = r_0$ one should mirror this spherical volume to one such that r goes from r_0 to a . Additionally, one must join to each copy the desired external spacetime from a to ∞ , ensuring continuity at $r = a$.

This Lorentzian metric lead us to the following Riemannian metric:

$$dt^2 = e^{-2\Phi} \left(d\tau^2 + \frac{dr^2}{1 - \frac{b(r)}{r}} + r^2 d\Omega^2 \right). \quad (55)$$

We will now explore an example presented in [3] where it is considered a matching of an interior solution with an exterior Schwarzschild solution ($\tau_{ext} = 0$ and $\Lambda_{ext} = 0$) and with zero tangential pressure at the junction. Under these circumstances, [3] states that for a wormhole of unitary mass, $m = 1$, $b(a) = 2$. Choosing

$$\Phi(r) = \Phi_0, \quad (56)$$

$$b(r) = (r_0 r)^{\frac{1}{2}}, \quad (57)$$

We have $b(a) = (r_0 a)^{\frac{1}{2}}$, and so the matching happens at $a = \frac{4}{r_0}$. Imposing continuity at $r = a$, the interior metric, $r_0 \leq r \leq a$, is given by

$$ds^2 = - \left(1 - \sqrt{\frac{r_0}{a}} \right) dt^2 + \frac{dr^2}{\left(1 - \sqrt{\frac{r_0}{r}} \right)} + r^2 d\Omega^2, \quad (58)$$

and the exterior metric, $a \leq r \leq \infty$, is given by

$$ds^2 = - \left(1 - \frac{\sqrt{r_0 a}}{r} \right) dt^2 + \frac{dr^2}{\left(1 - \frac{\sqrt{r_0 a}}{r} \right)} + r^2 d\Omega^2, \quad (59)$$

which lead us to the following Riemannian surface:

$$\begin{cases} dt^2 = \left(1 - \sqrt{\frac{r_0}{a}} \right)^{-1} \left[d\tau^2 + \left(1 - \sqrt{\frac{r_0}{r}} \right)^{-1} dr^2 + r^2 d\Omega^2 \right] & , \quad r_0 \leq r \leq a \\ dt^2 = \left(1 - \frac{\sqrt{r_0 a}}{r} \right)^{-1} \left[d\tau^2 + \left(1 - \frac{\sqrt{r_0 a}}{r} \right)^{-1} dr^2 + r^2 d\Omega^2 \right] & , \quad a \leq r \leq \infty \end{cases} \quad (60)$$

4.6 Radial Motion

Focusing on radial motion, setting $d\theta = d\phi = 0$ and defining ρ and z such that: $\rho^2 = \left(1 - \sqrt{\frac{r_0}{a}} \right)^{-1}$ and $d\rho^2 + dz^2 = \rho^2 \left(1 - \sqrt{\frac{r_0}{r}} \right)^{-1} dr^2$, for $r_0 \leq r \leq a$, and $\rho^2 = \left(1 - \frac{\sqrt{r_0 a}}{r} \right)^{-1}$ and $d\rho^2 + dz^2 = \rho^4 dr^2$, for $a \leq r \leq \infty$. For the values of r_0 and a previously presented, one obtains the surface depicted in figure 9.

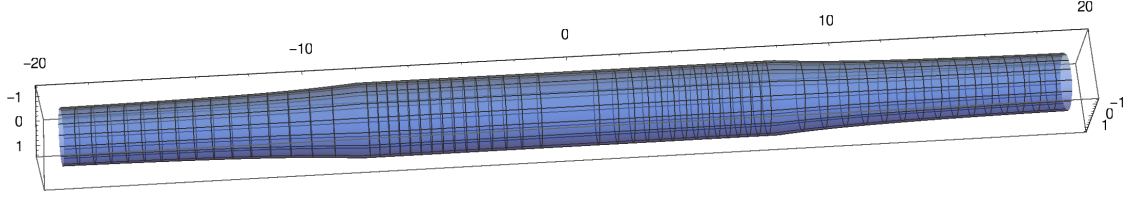


Figure 9: Wormhole ; $d\theta = d\phi = 0$

Looking at the plot, one may conclude that the exterior region is the same as the one obtained in section 3.1. However, the interior is a flat cylinder. This arises from the choice of $\Phi = \Phi_0$, which lead to $\rho = \text{const.}$ for $r_0 \leq r \leq a$. This means that the region inside the wormhole is one of constant potential.

Regarding motion of light rays, null geodesics do not curl around the surface and thus match the black straight lines. These lines simply go through the wormhole. On the other hand, geodesics that match the motion of massive particles are those that curl around the surface. These may start outside, enter the wormhole and finally leave it the same way they entered. Notwithstanding, if one stops this motion inside the wormhole, then the orbit becomes a circular one, $dr = 0$, and thus it will stand still inside the wormhole. Besides, since the interior of the wormhole is a region of constant potential, both particles and light beams move at constant velocity, $d\rho = 0$ and $\frac{dz}{dt}$ and $\frac{dr}{dt}$ are both constant.

ACKNOWLEDGEMENTS

I would like to acknowledge the Calouste Gulbenkian Foundation for funding the program "Novos Talentos em Matemática" and thus give me the opportunity to develop this research project.

Finally, I would like to express my gratitude to my tutor, professor José Natário, for his support and enthusiastic guidance.

REFERENCES

- [1] Marco Cariglia and Filipe Kelmer Alves. The Eisenhart lift: a didactical introduction of modern geometrical concepts from Hamiltonian dynamics. *Eur. J. Phys.*, 36(2):025018, 2015.
- [2] L.C. Epstein. *Relativity Visualized*. Taylor & Francis, 1984.
- [3] Jose' P. S. Lemos, Francisco S. N. Lobo, and Sergio Quinet de Oliveira. Morris-Thorne wormholes with a cosmological constant. *Phys. Rev.*, D68:064004, 2003.
- [4] V. Perlick and Springer-Verlag. *Ray Optics, Fermat's Principle, and Applications to General Relativity*. Lecture Notes in Physics Monographs. Springer, 2000.
- [5] Bernard F. Schutz. *A FIRST COURSE IN GENERAL RELATIVITY*. Cambridge Univ. Pr., Cambridge, UK, 1985.
- [6] Irwin I. Shapiro. Fourth test of general relativity. *Phys. Rev. Lett.*, 13:789–791, Dec 1964.